Gépészet 2008
Budapest, 29-30.May 2008.

G-2008-E-10

HIGH RESOLUTION VELOCITY MEASUREMENTS UPSTREAM AND DOWNSTREAM OF AN AXIAL FLOW FAN ROTOR

Cs. Horváth
Ph.D. student, Department of Fluid Mechanics, Budapest University of Technology and Economics,
H-1111 Budapest, Bertalan Lajos utca 4-6. Tel: (1) 463-2546, email: horvath@ara.bme.hu

J. Vad
Associate Professor, Department of Fluid Mechanics, Budapest University of Technology and Economics,
H-1111 Budapest, Bertalan Lajos utca 4-6. Tel: (1) 463-2464, email: horvath@ara.bme.hu

Abstract: An important topic of research at The Budapest University of Technology and Economics, Department of Fluid Mechanics is that of axial flow fans of controlled vortex design. In this ongoing research, a computational fluid dynamics simulation has been developed for the further investigation of the flow phenomena developing in the vicinity of the rotor. In order to fully validate this simulation, detailed velocity measurements have been carried out on the flow both upstream and downstream of a rotor designed using a controlled vortex design method incorporating circumferential forward skew. These measurements have already been used in order to validate the pitchwise averaged data of the computational fluid dynamics simulation, with this article focusing on the validation of the pitchwise resolved data.

Keywords: *Turbomachinery, Validation, Controlled vortex design, Computational fluid dynamics.*

1. INTRODUCTION

Axial flow fans of controlled vortex design have been a topic of research at the Budapest University of Technology and Economics, Department of Fluid Mechanics for many years [1-6]. A computational fluid dynamics (CFD) simulation has been developed (Figures 1-2) in order to further the efforts made toward better understanding the flow phenomena developing in the vicinity of the rotor [4-5]. In order to fully validate this simulation, detailed velocity measurements from both upstream and downstream of a rotor designed using a controlled vortex design method incorporating circumferential forward skew [5, 7] are used here to validate the pitchwise resolved data (Figure 2). These measurements have already been used in order to validate the pitchwise averaged data of the CFD simulation [5, 8].

While the classic free vortex design concept is based on a prescription of spanwise constant blade circulation, for which a two-dimensional (2-D) blade design methodology can be applied as a reasonable approximation, the controlled vortex design is based on a prescription of increased blade circulation along the span of the blade, which results in three-dimensional (3-D) flow phenomena developing in the blade passage and the wake [6, 9]. Therefore the applicability of 2-D cascade data alone is questionable during the design process. The use of 3-D CFD simulations can provide a means for fully understanding the interblade flow phenomena, so that the design methodology of controlled vortex design rotors can be further improved.

In the validation of the CFD simulations in this paper, measurements were conducted on the rotor of the open-type low-speed wind tunnel facility of the Hungarian Institute of Agricultural Engineering, Gödöllő, Hungary (Figure 2). This test facility, including the rotor, was designed at the Department of Fluid Mechanics. The rotor is of controlled vortex design with circumferential forward skew. The design specifications of the rotor are reported in [5]. The measurements were conducted in two planes, one being 74.5% axial chord length upstream of the leading edge of the rotor and the other being 26.6% axial chord length downstream of the trailing edge of the rotor, measured at midspan. A detailed description of the measuring equipment and the procedure can be found in [5, 7-8].

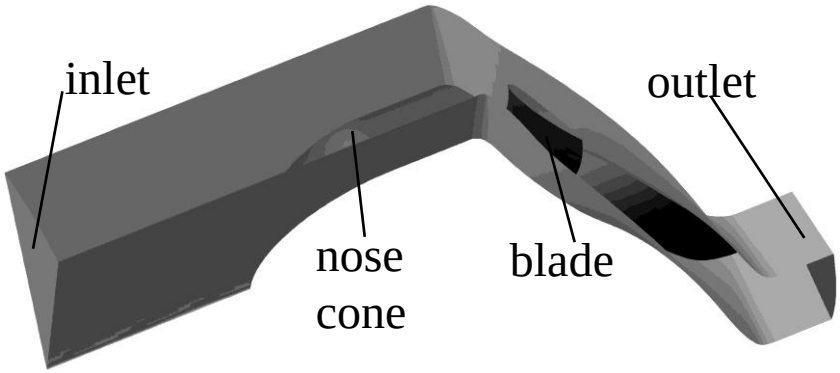

FIG. 1. Computational domain [5]

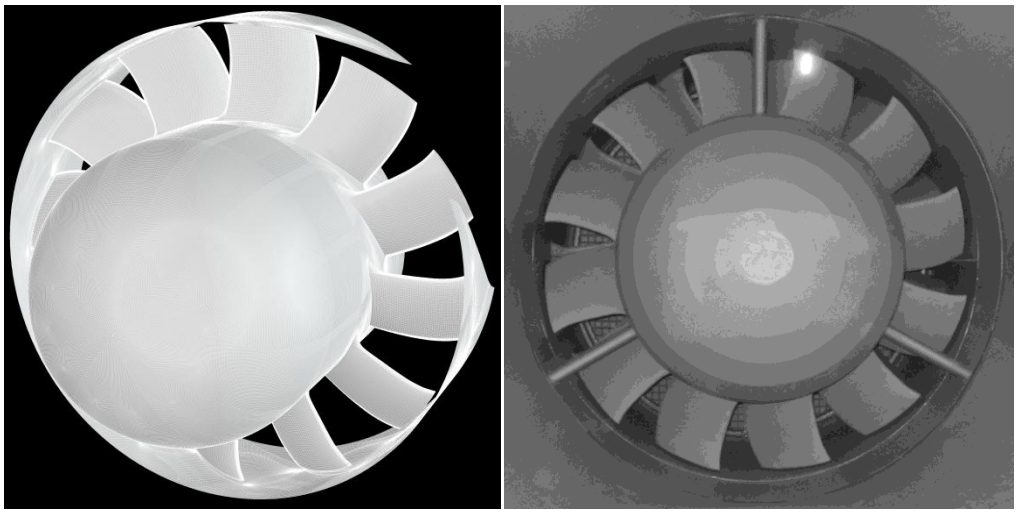

FIG. 2. Virtual axonometric view of the simulation model (left)
and photo of the actual rotor (right) [5]

In the validation of the pitchwise averaged CFD data, the measurements conducted at various radii were time-averaged. In this way an average was taken of 300000 data points resulting from the 15 $[s]$ long measurement conducted at 20 $[kHz]$. In the evaluation of the pitchwise resolved data, a position signal was used to divide the 104 revolutions worth of data into single blade passage segments. These segments were then averaged. In this way an average blade passage was created in which the flows in the two examined planes could be compared with the results found in the same planes of the CFD simulation.

2. COMPARING THE MEASUREMENTS TO THE LITERATURE

The first step in validating the CFD with the measurement results is to understand the physics of the flow seen in the measurement results. In order to do this, the local axial flow coefficient, φ, the local ideal total pressure rise coefficient, ψ_{id} and the local radial flow coefficient, φ_r were examined. These results were investigated in both of the examined measurement planes, with the design condition results being presented here. The contour plots represent the fan section which would be seen above the fan hub when looking at the fan from upstream (see Figures 3-8).

In first of all examining the downstream results of the local axial flow coefficient for the design condition, φ_{2D}, many flow characteristics which are typical of axial flow turbomachinery of controlled vortex design can be witnessed (Figure 3). It is known that the fan blades are rotating from right to left in the contour plots (as indicated by the arrows), which results in the left side of the plots showing the pressure side (PS) data, and the right side showing the suction side (SS) data, with the blade being located between the two. It is evident, that since these measurements were taken downstream of the rotor, the actual blade is not seen in the plot, but its wake. It can be seen in all the plots for the measured data that the results are presented as being laid out on a square plane as a result of the measurement technique. It can also be seen in the measurement data that there is an area along the top and the bottom of each plot which does not show data. These are the areas near the hub and the casing, where measurements could not be made.

In examining these results for those characteristics which have been reported in the literature, it can be seen that there is a reduced axial velocity in the blade wake (W) [2]. A blade root suction side stall (ST) zone can be seen as a thickening of the wake near the hub [2]. The presence of a passage vortex trace (PV) was observed [2, 10], which can be found in the hub boundary layer, near the suction side of the blade. The increase in axial velocity on the suction side of the blade was also in accordance with the literature [2], which states that the increase in axial velocity is a result of the blockage effect of the suction side boundary layer. In examining the flow near the casing, it can be seen that there is a lag in axial velocity along the casing wall (C) [2]. This area is larger on the pressure side and smaller on the suction side of the rotor tip (T). The leakage flow from the adjacent blade accumulates on the pressure side of the blade [11].

In looking at the design condition results of the local ideal total pressure rise coefficient downstream of the rotor, $\psi_{id\,2D}$, in Figure 4, it can be seen that there is a low relative kinetic energy zone accumulating near the rotor tip of the pressure side [2], which can be characterized by a moderated axial velocity and increased absolute tangential velocity. This zone has an increase in tangential velocity, as the leakage flow from the adjacent blade accumulates on the pressure side of this blade [11], which is the reason why the $\psi_{id\,2D}$ value is so large here, and why the φ_{2D} is so small in this area.

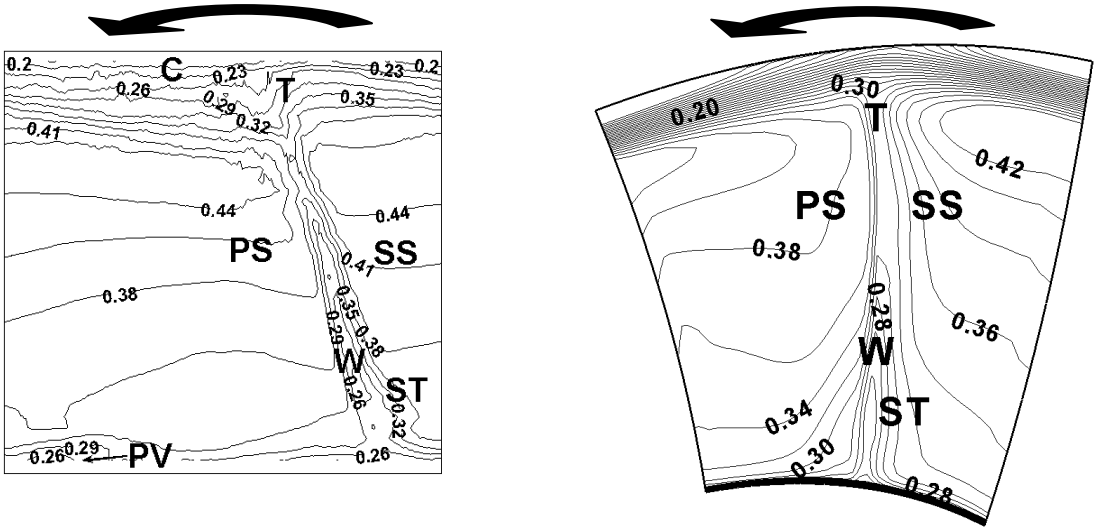

Fig. 3. φ_{2D}. Left column: measured data, Right column: CFD data

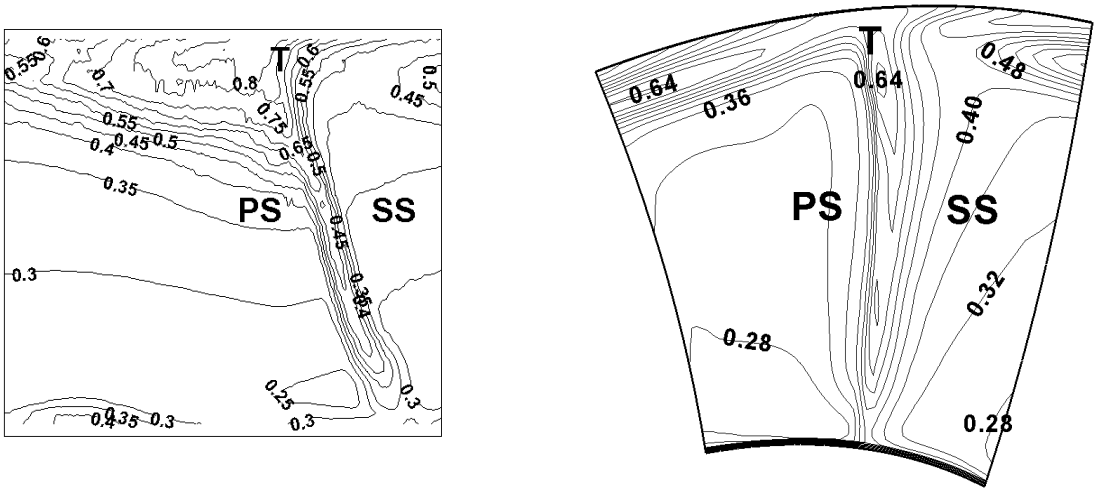

Fig. 4. $\psi_{id\ 2D}$. Left column: measured data, Right column: CFD data

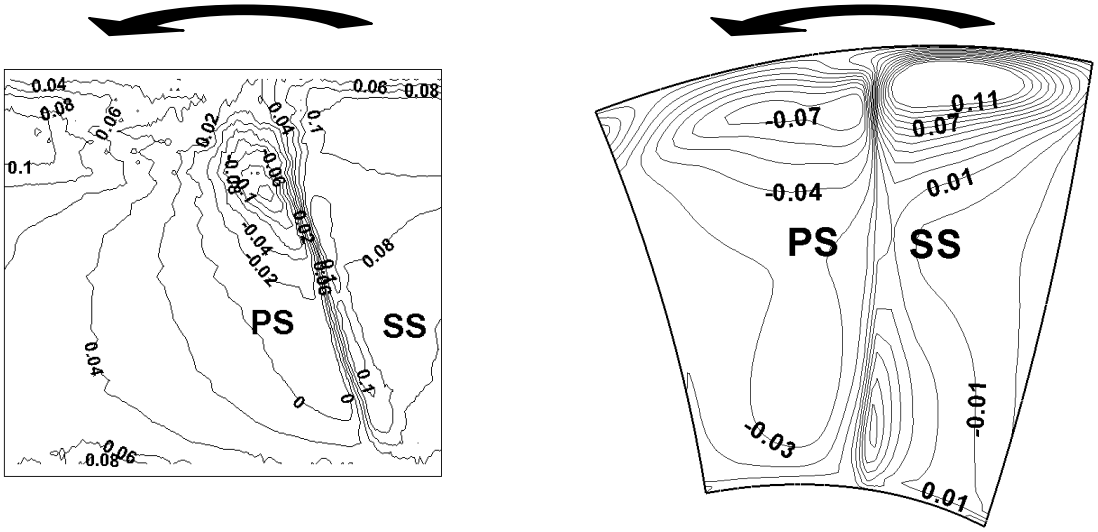

Fig. 5. $\varphi_{r\ 2D}$. Left column: measured data, Right column: CFD data

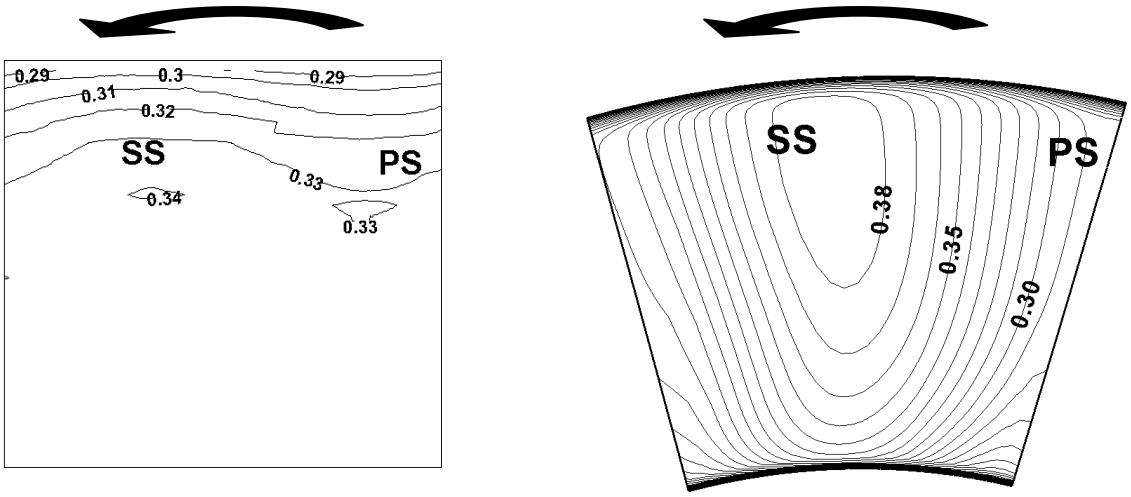

Fig. 6. φ_{1D}. Left column: measured data, Right column: CFD data

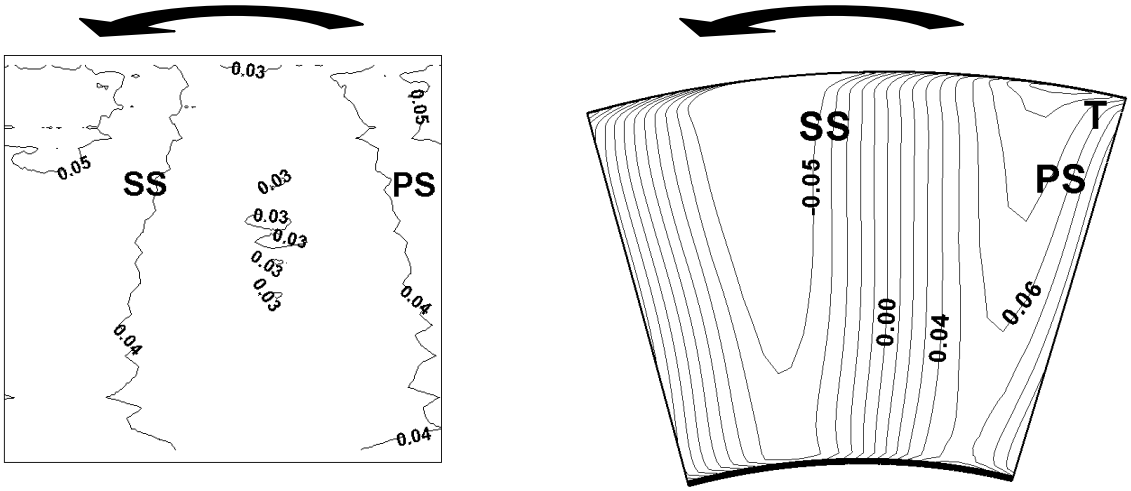

Fig. 7. $\psi_{id\ 1D}$. Left column: measured data, Right column: CFD data

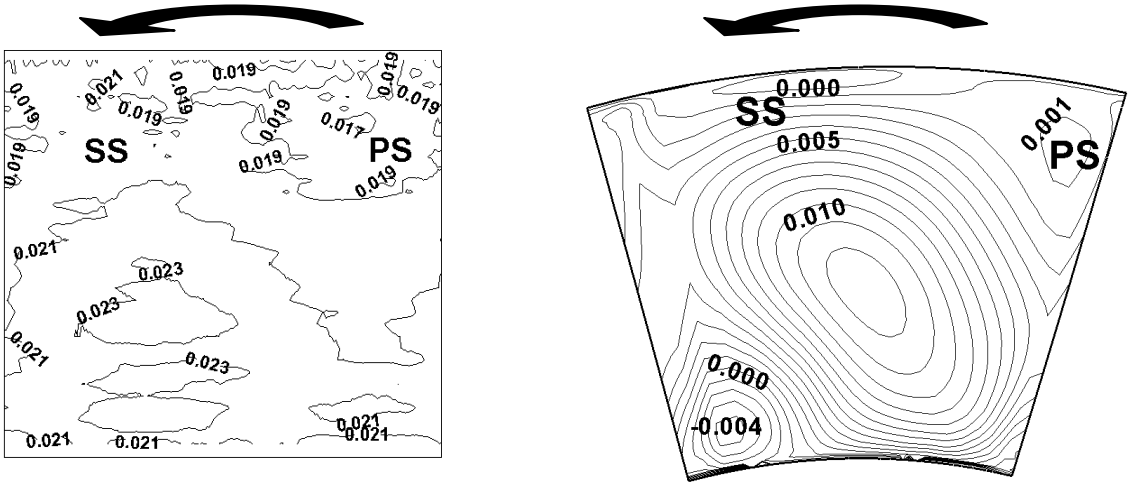

Fig. 8. $\varphi_{r\ 1D}$. Left column: measured data, Right column: CFD data

The third dimensionless value to be examined downstream of the rotor is the local radial flow coefficient for the design condition, $\varphi_{r\ 2D}$. When examining the φ_{2D}, $\psi_{id\ 2D}$ and

the $\varphi_{r\,2D}$ together in Figures 3-5, the characteristic 3-D secondary flow for rotors of controlled vortex design, which fills the blade passage, can be seen. This characteristic flow is a result of the spanwise gradient for the ideal total head rise, and thus also for the blade circulation, which is used in the controlled vortex design technique [1-2, 12]. The shed vortices resulting from this blade design technique cause a 3-D flow to develop in the blade passage, which can be seen in the inward flow toward the hub on the pressure side and the outward flow on the suction side of the blade wake in the $\varphi_{r\,2D}$ results [6].

Upstream of the rotor, the same dimensionless numbers can be examined as were looked at downstream. In Figure 6 the upstream local axial flow coefficient for the design condition, φ_{1D}, shows the upstream effects of the rotor on the axial flow. Though little was found in the literature regarding the flow upstream of a rotor of controlled vortex design, it can be seen that the flow on the suction side of the rotor shows a slight increase in axial velocity as compared to the pressure side, just as was seen downstream of the rotor. Therefore the suction effect on the suction side corresponding to the higher mean velocity on the suction side acts forward to the inlet flow field, resulting in a locally increased axial velocity. It should be noted here that the upstream figures are looked at from the same viewpoint as the downstream results. This is brought to the readers' attention in order to avoid any confusion which might be caused by the positioning of the suction side marker being on the left side of the figure. This is due to the rotational affect of the rotor on the fluid which propagates a certain distance upstream and downstream of the rotor.

The design condition results for the upstream local ideal total pressure rise coefficient, $\psi_{id\,1D}$, in Figure 7 presented only a small variation in value as did the results for φ_{1D}. It can be seen though that there is a small increase in the tangential velocity near the rotor tip, as was seen downstream of the rotor.

The third dimensionless value to be examined upstream of the rotor, in Figure 8, is the local radial flow coefficient for the design condition, $\varphi_{r\,1D}$. In these results, it can be seen that the nose cone forces the flow out from the center of the inlet cross-section. This can be seen in the higher values for the $\varphi_{r\,1D}$ near the hub [2]. It can also be seen that the flow originating from the non-free vortex design, which causes a vortical flow inside the blade passage, also influences the flow upstream of the rotor. This can be seen in the slightly decreased radial outward flow on the pressure side and the slightly increased radial outward flow on the suction side of the rotor, just as was experienced downstream of the rotor.

3. EVALUATION OF THE MEASUREMENT ERROR

The second step in evaluating the results of the measurements is to determine the measurement error and the limitations of the measurement, in order to determine the validity of the results reached during the evaluation of the CFD. Being that the measurements were carried out in an industrial environment, and not in a turbomachinery test facility, where the conditions would be more ideal, the hot-wire anemometry measurements have many limitations. The results of the uncertainty analysis for the measurement have been presented in [5], where it can be seen that the sources of the error were traced back to the errors arising from the calibration of the hot wire, those resulting from the equipment used for the measurements, those which resulted from the variations in the environmental conditions during the execution of the measurements, and those arising from the uncertainties in the positioning of the equipment. The absolute error of the measured results do not exceed ± 0.015 for φ_{2D}, ± 0.028 for $\psi_{id\,2D}$, ± 0.004 for $\varphi_{r\,2D}$, ± 0.012 for φ_{1D}, ± 0.002 for $\psi_{id\,1D}$ and ± 0.001 for $\varphi_{r\,1D}$.

It was found in the validation of the pitchwise averaged data of the CFD simulations that the results did not show an exact agreement with those obtained in the measurement, even

when taking into consideration the calculated errors. In examining the source of this disagreement, it was found that the measurement results have some limitations due to the oscillation of the flow direction caused by the passing of the blades. In using two-component cross wire probes for measuring three-dimensional flow, it is necessary that the out of plane component of the velocity, which is perpendicular to the measuring plane, be small compared to the in plane flows [13]. In practice, this necessitates that α, the angle between the probe axis and the absolute velocity vector, of the measurements being taken perpendicularly to the investigated measurements have a value of less than $\pm 10°$ [14]. These conditions were not fulfilled in a large part of the domain of the downstream measurements, though a recently conducted measurement at the Department of Fluid Mechanics demonstrated that for up to a $\pm 17°$ variation of α, the measurement error was less than 6%, which is better than what was expected by the authors. In examining the values of α in Figures 9-12, it can be seen that there are areas where the values exceed these limits. Therefore it needs to be taken into consideration that the velocity values (quantitative data) measured in the perpendicular plane have to be treated with criticism when the value of α is greater than $\pm 10°$, due to the affect of the out of plane flow, though this does not influence the validity of the qualitative discussion presented herein.

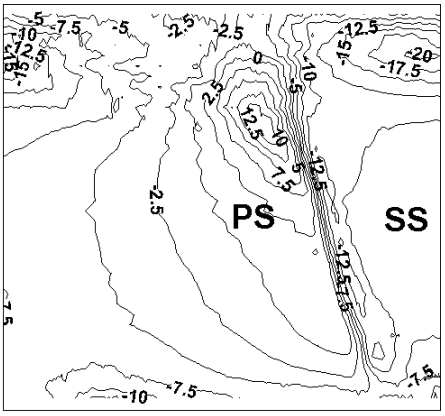

FIG. 9. α values measured in the axial-radial measurement plane downstream of the rotor, affecting the values of φ_{2D} and $\psi_{id\ 2D}$.

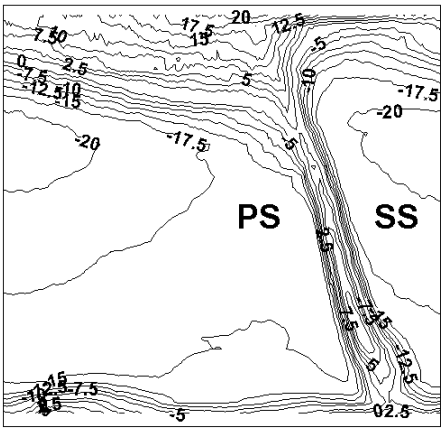

FIG. 10. α values measured in the axial-tangential measurement plane downstream of the rotor, affecting the value of $\varphi_{r\ 2D}$.

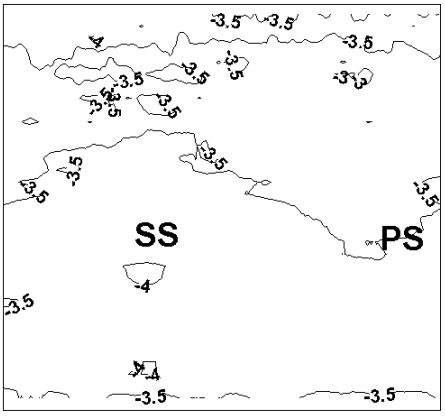

FIG. 11. α values measured in the axial-radial measurement plane upstream of the rotor, affecting the values of φ_{1D} and $\psi_{id\ 1D}$.

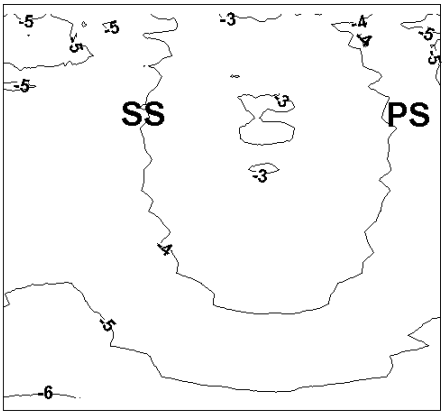

FIG. 12. α values measured in the axial-tangential measurement plane upstream of the rotor, affecting the value of $\varphi_{r\ 1D}$.

4. VALIDATION OF THE CFD DATA

In making qualitative comparisons between the measured and the CFD data [5], the different flow phenomena, which were realized in the investigation of the measurement data, are looked for in the CFD results. In first of all examining the downstream results for φ_{2D} in Figure 3, the presence of the reduced axial velocity can easily be seen in the blade wake. Though the average thickness of blade wake is thicker in the CFD, it can be seen that the blade wake is thicker near the hub as compared to the midspan, just as in the measurement results, with the minimal value being found in this area. This thickened blade wake is also an indicator of the suction side stall, which was seen in the measurement results. The passage vortex trace which was observed in the measurements cannot be seen here. It is also worth mentioning that the axial velocity on the suction side of the blade wake is not much higher than that on the pressure side, which is in accordance with the reasoning in [2], which states that the increase in axial velocity is a result of the blockage effect of the suction side boundary layer, which was not realized to a great extent, with the pressure vortex trace not being present in the results. The casing wall shows many of the same characteristics in the CFD results as can be seen in the measurements. The axial velocity is reduced, with a slightly

larger area of reduced axial velocity being visible on the pressure side of the rotor tip, where the leakage flow from the adjacent blade is accumulating [11]. It can be seen in the comparison of the results for φ_{2D}, that the differences between the characteristics of the measured and the simulated flows come from the inability of the simulation to precisely simulate the boundary layer flow. This can be seen here in the comparison of the blade wake as well as the hub and casing boundary layer results. The referenced literature [15-18] suggests the use of the standard k-ε turbulence model [19] for such investigations, and it was also found that among the two-equation turbulence models available in FLUENT [20], this one gave the results which best agreed with those from the measurements [5]. But while it can be seen throughout the validation that many of the characteristics which are seen in the measurement results, and supported by the literature, are found in the CFD results, there are some which are not. This will be seen as a reoccurring source of disagreement throughout the investigation.

The $\psi_{id\ 2D}$ CFD results in Figure 4 seem to show the area where the leakage flow from the adjacent blade is accumulating, characterized by a large $\psi_{id\ 2D}$ near the casing, as being composed of two small areas. One part can be seen in the wake of the rotor tip, with the other part being found along the casing wall, approximately in the middle of the blade passage. These results deter from those found in the measurement, where only one large value of $\psi_{id\ 2D}$ can be found on the pressure side of the rotor tip. In the CFD, not only the size of the area but the magnitude of $\psi_{id\ 2D}$ is smaller than in the measurements, where the two zones are seen as one larger zone. This is again a result of the turbulence modeling problems which were explained earlier.

In looking at the diagrams of $\varphi_{r\ 2D}$ in Figure 5, it was found that the CFD results show a larger area of the blade passage as experiencing an inward flow on the pressure side of the blade wake than in the measurement results. Though these results do not entirely agree with those found in the measurements, it does show that the characteristic 3-D secondary flow, which is resulting from the non-free vortex design, is successfully represented in the simulation.

The comparison of the upstream results show that the suction side effect of the rotor, increasing the axial velocity in the blade passage and thus slightly sucking the flow upstream of the rotor, can be realized in the φ_{1D} results of the CFD, as it was in the measurements (Figure 6). It can be seen that the peak value is located in generally the same area for both the CFD and the measurement, though the measurement results show a smaller value. The boundary layer problems can also be seen in the φ_{1D} results, since the measurement results show a larger area of decreased axial velocity in the casing boundary layer. The hub boundary layer results also deter from those found in the simulation, though that is dedicated to the differences between the modeled and the realized inlet geometries of the nose cone [5] (see Figure 2). The similarities between the CFD and the measurements can also be seen in the $\psi_{id\ 1D}$ results presented in Figure 7, in which it can be seen that the near rotor tip increase in tangential velocity also affects the flow upstream of the rotor, though the variation of the CFD results differ from those experienced in the measurement. It can also be seen in the hub boundary layer of the CFD results that the no slip condition gives the flow a large tangential velocity component. In comparing the $\varphi_{r\ 1D}$ results to those found in the measurements (Figure 8), it can be seen that the effect of the 3-D secondary flow resulting from the non-free vortex design can be found in the simulation, though the effect of the nose cone, causing a radial outward flow, cannot be seen as clearly. This is also an effect which should be seen in the boundary layer of the model, though here the differences between the geometries of the measured and the simulated nose cone could also cause deviations in results, as was stated earlier (Figure 2).

In the investigation of the validity of the CFD simulation of an axial flow fan of controlled vortex design, it was found that the simulation qualitatively resolves most of the characteristics which were found in the measurements and supported by the literature. The only characteristics which were not well resolved in the CFD results were those which would be found in the boundary layer. Though it is known that there is a measurement error which needs to be taken into consideration in comparing the data, it has been realized that the differences between the characteristics of the flow are a result of the standard k-ε turbulence model, which was used in the simulation along with the enhanced wall treatment of FLUENT. This turbulence model was referenced from [15-18], and was also found to give the most reasonable agreement with the measurement results in [5], from the two-equation turbulence modeling options built into FLUENT.

5. CONCLUSION

In the ongoing research at the Department of Fluid Mechanics of axial flow fans of controlled vortex design, a CFD simulation was developed for the further investigation of the flow phenomena developing in the vicinity of the rotor. This simulation was validated using high resolution velocity measurements, which were first compared to the literature. In this way it was found, which of the characteristic flows expected in the flow field of an axial flow fan of controlled vortex design with circumferential forward skew were resolved in the simulation. A good agreement was found between the CFD and the measurements, with the effect of the 3-D secondary flow resulting from the non-free vortex design method, the blade wake, and the suction side increase of the axial velocity being well depicted in both the upstream and the downstream results, while some of the other characteristics which were expected in the vicinity of the boundary layer, or as a result of some boundary layer phenomena, were not found. This comes as a result of the standard k-ε turbulence model, which was used in the simulation, and urges the introduction of a non-isotropic turbulence model before the intended future use of the simulation in acoustical investigations. In summarizing the results, it is promising that this simulation will provide a good tool for continuing the investigation of turbomachinery of controlled vortex design.

ACKNOWLEDGEMENTS

This work has been supported by the Hungarian National Fund for Science and Research under contract No. OTKA K63704. Gratitude is expressed to ARA Kwedikha for providing the simulation results and to M Balczó for his measurement expertise.

NOMENCLATURE

d diameter
n rotor speed
r radius $= d/2$
R dimensionless radius $= r/r_t$
$\mathrm{u_{ref}}$ reference velocity $= \mathrm{d_t \pi n}$
v flow velocity in the absolute frame of reference
$\Delta p_{\mathrm{tot\,id}}$ rotor ideal total pressure rise
α angle between the probe axis and the absolute velocity vector
ρ density
φ local axial flow coefficient $= \mathrm{v_x} / \mathrm{u_{ref}}$
φ_r local radial flow coefficient $= \mathrm{v_r} / \mathrm{u_{ref}}$
ψ_{id} local ideal total pressure rise coefficient $= \Delta \mathrm{p_{tot\,id}} / \left(\rho \mathrm{u_{ref}^2} / 2\right) = 2\mathrm{Rv_u} / \mathrm{u_{ref}}$ (from the Euler equation of turbomachines, considering swirl-free inlet far upstream)

SUBSCRIPTS

D design; at the design flow rate
id ideal (inviscid)
r radial coordinate
t blade tip
tot total
u tangential coordinate
x axial coordinate
1 rotor inlet plane
2 rotor exit plane

REFERENCES

[1] Vad J, Bencze F. Three-dimensional flow in axial flow fans of non-free vortex design. Int Jnl of Heat and Fluid Flow 1998: 19: 601-607.
[2] Corsini A, Rispoli F, Bencze F, Vad J. Concerted experimental and numerical studies on axial flow fan rotor aerodynamics. IMechE paper 1999: C557/106/99. In: 3rd European Conference on Turbomachinery Fluid Dynamics and Thermodynamics. London: 1999. p. 519-531.
[3] Vad J, Csonka Sz, Bencze F. Experimental and numerical investigation of axial flow rotor inlet condition. In: microCAD conference. Miskolc: 1999. p. 175-180.
[4] Vad J, Kwedikha ARA, Horváth Cs. Combined effects of controlled vortex design and forward blade skew on the three-dimensional flow in axial flow rotors. In: Conference on Modeling Fluid Flow (CMFF'06). Budapest: 2006. p. 1139-1146.
[5] Vad J, Kwedikha ARA, Horváth Cs, Balczó M, Lohász MM, Régert T. Aerodynamic effects of forward blade skew in axial flow rotors of controlled vortex design. Proc Instn Mech Engrs, Part A, Jnl Power and Energy 2007: 221(A):1011-1023.
[6] Vad J, Horváth Cs. The impact of the vortex design method on the stall behavior of axial flow fan and compressor rotors. In: ASME Turbo Expo 2008: Power for Land, Sea and Air. Berlin: 2008. (accepted).
[7] Horváth Cs, Vad J. Development and application of a multi-component hot wire measuring system. In: Fifth Conference on Mechanical Engineering, Gépészet 2006. Budapest: 2006. CD-ROM ISBN 963 593 465 3.

[8] Horváth Cs, Vad J. Validation of a CFD simulation using a multi-component hot wire measurement. In: microCAD conference. Miskolc: 2007. p. 661-66.
[9] Gallimore SJ, Bolger JJ, Cumpsty NA, Taylor MJ, Wright PI, Place JM. The use of sweep and dihedral in multistage axial flow compressor blading. - Parts I and II. ASME Jnl Turbomachinery 2002: 124: 521-541.
[10] Sieverding CH. Secondary Flow in Axial Turbines, Lecture note No. 9. Brussels: Von Karman Institute for Fluid Dynamics 1986.
[11] McNulty GS, Decker JJ, Beacher, BF, Khalid SA. The impact of forward swept rotors on tip-limited low-speed axial compressors. ASME Paper 2003: GT2003-38837.
[12] Dring RP, Joslyn HD, Hardin LW. An investigation of axial compressor rotor aerodynamics. ASME Jnl Engineering Power 1982: 104: 84-96.
[13] Bruun HH. Hot-Wire Anemometry, Principles and Signal Analysis. New York: Oxford University Press Inc. 2002.
[14] Podboy G. (2006). (NASA Glenn Research Center), *private communication.*
[15] Beiler MG. Untersuchung der dreidimensionalen Strömung durch Axialventilatoren mit gekrümmten Schaufeln. Doctoral Dissertation, Universität-GH-Siegen, VDI Verlag Düsseldorf, Reihe 7: Strömungstechnik, Nr. 298, 1996.
[16] Beiler MG, Carolus TH. Computation and measurement of the flow in axial flow fans with skewed blades. ASME Jnl Turbomachinery. 1999: 121: 59-66.
[17] Govardhan M, Krishna Kumar OG, Sitaram N. Computational study of the effect of sweep on the performance and flow field in an axial flow compressor rotor. Proc Instn Mech Engrs, Part A, Jnl Power and Energy 2007: 221(A): 315-329.
[18] Benini E, Biollo R. On the aerodynamics of swept and leaned transonic compressor rotors. ASME paper 2006: GT2006-90547.
[19] Launder BE, Spalding DB. Lectures in mathematical models of turbulence. London: Academic Press 1972.
[20] Fluent 6.2.16 user's guide, 2004 (Fluent Inc., Lebanon, NH, USA).